

SUPPLEMENTAL DATA SECTION

Supplementary Methods

LC-MS/MS on a Thermo Scientific LTQ Orbitrap Elite spectrometer

The analysis described here and the following two sections were performed by the Keck Protein Microchemistry Facility at Yale University on a fee basis. LC-MS/MS analysis was performed on a Thermo Scientific LTQ Orbitrap Elite with a Waters nanoAcquity UPLC system, and uses a Waters Symmetry® C18 180µm x 20mm trap column and a 1.7 µm, 75 µm x 250 mm nanoAcquity™ UPLC™ column (35°C) for peptide separation. Trapping is done at 15µl/min, 99% Buffer A (100% water, 0.1% formic acid) for 1 min. Peptide separation is performed at 300 nl/min with Buffer A: 100% water, 0.1% formic acid and Buffer B: 100% acetonitrile, 0.075% formic acid. A linear gradient (53 minutes) is run with 5% buffer B at initial conditions, 50% B at 48 minutes, and 85% B at 53 minutes. MS was acquired in the Orbitrap part of the instrument (400-2000 m/z) using 1 microscan and a resolution of 30,000. MS/MS was also acquired in the Orbitrap using CID for up to 15 MS masses per MS scan. The data was searched using Mascot Distiller and the Mascot (Matrix Science) search algorithm for the protein identification runs.

Label-free quantitation (LFQ) data analysis

The Progenesis LCMS software (Nonlinear Dynamics, Ltd.) performs feature/peptide extraction, chromatographic/spectral alignment, data filtering, and statistical analysis. First, the raw data files are imported into the program. A sample run is then chosen as a reference (usually at or near the middle of all runs in a set), and all other runs are automatically aligned to that run in order to minimize retention time (RT) variability between runs. (note that due to the very high reproducibility of the nanoACQUITY, the RT shifts are very minimal if at all). No adjustments are necessary in the m/z dimension due to the high mass accuracy of the mass spectrometer (typically <3ppm). All runs are selected for detection with an automatic detection limit. Features within RT ranges of 0-10 minutes are often filtered out, as are features with charge $\geq +6$ and +1. Progenesis calculates a normalization factor for each run to account for differences in sample load between injections, and differences in ionization. The normalization factor is determined by calculating a quantitative abundance ratio between the reference run and the run being normalized. The basic assumption is that most proteins and therefore peptides are not changing in the experiment so the quantitative value should equal 1. The experimental design is setup to group multiple injections from each run. The algorithm then calculates tabulated raw and normalized abundances, max fold change, and Anova values for each feature in the data set. The MS/MS spectra (a combined list of all LC-MS/MS runs) are exported to an .mgf (Mascot generic file) for database searching. The Mascot search results are exported to an .xml file using a significance cutoff of $p < 0.05$ and are then imported into the Progenesis LCMS software, where search hits are assigned to corresponding features or peptides. The features are tagged in sets based on characteristics such as MSMS>1, $p < 0.05$. Additional features or peptides can be identified by re-running the sample using an exclude list of the identified proteins. Using the Mascot database search algorithm, the Keck Facility considers a protein identified when Mascot lists it as significant and more than 2 unique peptides match the same protein. The Mascot significance score match is based on a MOWSE score and relies on multiple matches to more than one peptide from the same protein.

Protein identification and database searching

All MS/MS spectra were searched in-house using the Mascot (Matrix Science) algorithm (current version 2.4.0) for un-interpreted MS/MS spectra after using the Mascot Distiller or Progenesis LC-MS software (Nonlinear Dynamics Ltd) to generate Mascot compatible files. Search parameters used for searching were N α -terminal acetylation, initiator methionine removal, methionine oxidation and acrylamide modified cysteine, a peptide tolerance of ± 10 ppm, MS/MS fragment tolerance of ± 0.2 Da, and peptide charges of up to +5. Normal and decoy (to determine the false discovery rates) database searches were run. Confidence level was set to 95% within the MASCOT search engine for protein hits based on randomness.

Three-dimensional model prediction for the Der1 protein using Phyre2 software

Using the web-based protein structure prediction tool, Phyre2, a structural model of the Der1 protein was generated based on the available structure of the bacterial GlpG protease (PDB 2IC8). 73% of the Der1 sequence was modeled onto the GlpG structure with a confidence score of 99.8%. MolProbity Ramachandran analysis (Chen et al., 2010) confirmed that 85.2% of Der1 residues were in favored regions and 92.9% of residues were in allowed regions.

SUPPLEMENTARY FIGURE LEGENDS

Supplementary Figure 1. Effect of NatB loss on the degradation of other Doa10 substrates. **A.** Weak stabilization of Ubc6, which lacks a NatB consensus sequence, in *nat3Δ* cells. Cycloheximide addition to block further protein synthesis marked the beginning of the chase period. An antibody against Ubc6 was used for immunoblotting. PGK served as a loading control. **B.** NatB is not required for degradation of Doa10 substrate Ste6*-HA. An antibody against the HA epitope was used for immunoblotting.

Supplementary Figure 2. Effects of NatB loss on Doa10 pathway components. **A.** Levels of the Doa10 ligase, a NatB (Nat3/Mdm20) substrate, are similar in WT and *nat3Δ* strains. Anti-Doa10 antibodies were used for immunoblotting. PGK, loading control. **B.** The Cue1 TM protein localizes to membranes in *nat3Δ* cells. Total yeast cell lysates (T) made in the absence of detergent were divided in membrane pellet (P) and soluble cytosolic (S) fractions by centrifugation and analyzed by immunoblotting with antibodies to the indicated proteins. Pmal served as a membrane protein marker, PGK as a cytosolic marker. **C.** Loss of NatB activity causes a slight increase in bulk ubiquitin conjugates. Whole cell extracts from strains of the indicated genotypes were evaluated by anti-ubiquitin immunoblotting. PGK, loading control. Migration of size standards (in kDa) is indicated on the left.

Supplementary Figure 3. Effect of NatB and NatA mutations on CPY* modification and degradation. **A.** CPY* glycosylation is unaffected by loss of NatB (Nat3/Mdm20). Extracts were either not treated (-) or treated (+) with Endoglycosidase H (EndoH; Roche) and subjected to anti-CPY immunoblot analysis. **B.** CPY* degradation is impaired in *MA-der1-HA nat1* but not *DER1-HA nat1* cells. The method of cell extraction (Kushnirov, 2000) was different from that used for Fig. 4, but the results were the same. The *nat1-4::LEU2* insertion allele was used to inactivate NatA (Arendt and Hochstrasser, 1997), and all cells had the endogenous *DER1* locus deleted; the “*der1Δ*” cells were transformed with an empty plasmid, while the other strains were transformed with plasmids expressing the indicated *DER1* or *der1* alleles. Transformants with endogenous WT *NAT1* were derived from MHY7110, those with *nat1-4::LEU2* from MHY7794.

Supplementary Figure 4. Purification and N-terminal acetylation analysis of the MA-Der1 protein. **A.** Purification of Flag-tagged MA-Der1 from strains of the indicated genotypes. The protein was excised from the Coomassie-stained gel, cleaved with trypsin, and analyzed by LC-MS/MS. **B.** Relative N α -acetylation levels of MA-Der1 in WT and mutant strains.

Supplementary Figure 5. N-terminal mutations of Der1 and their effects on ERAD-L in WT and N α -acetylation mutants. **A.** Mutation of the second residue of Der1 from Asp to Glu preserves Der1 function in ERAD-L as measured by CPY* degradation. Protein stability was assayed by cycloheximide chase for the indicated times and anti-CPY immunoblotting. PGK, loading control. **B.** The ME-Der1-HA protein is sensitive to loss of NatB for its function. CPY* degradation was measured by cycloheximide chase/anti-CPY immunoblotting. **C.** ML-Der1-HA supports ERAD-L even when its acetylation is blocked by loss of NatC (Mak3/Mak10/Mak31).

Degradation rates of both WT Der1-HA and ML-Der1-HA are increased in *mak3Δ* cells but this does impede CPY* degradation.

Supplementary Figure 6. Degradation of Der1 is mediated primarily by Hrd1. Low-copy plasmids expressing MD-Der1-HA (WT, top) and ML-Der1-HA (bottom) were transformed into cells of the indicated genotypes. WT, MHY1366; *nat3Δ*, MHY6920; *doa10Δ nat3Δ*, MHY6856, and *hrd1Δ nat3Δ*, MHY7430. The last strain is from the BY4741 background, the first three from the MHY501 background. Endogenous Der1 is present in all strains.

Supplementary Figure 7. Lack of Der1 acetylation does not influence Der1 dimerization or binding to Usa1. Anti-FLAG immunoprecipitation was followed by immunoblotting with the indicated antibodies. Note that Der1-FLAG is short-lived in these *HRD1* cells and was therefore undetectable in the inputs by either anti-Der1 or anti-FLAG immunoblotting. We consistently observed lower Der1 levels in the *nat3Δ* strain, whereas Usa1-3myc levels were increased. Endogenous Der1 is present in all strains. *, cross-reactive band.

Supplementary Figure 8. Membrane topology of the yeast Der1 protein in WT and *nat3Δ* cells. **A.** Topology analysis of Der1-Flag alleles with glycosylation sites inserted after the indicated residues. Cell lysates were left untreated or treated with EndoH to remove N-linked glycans and then analyzed by anti-Flag immunoblotting. **B.** Comparison of the original 4-TM model for Der1 and a possible 6-TM topology. **C.** Possible 6-TM structure of the Der1 protein. Bioinformatic analysis (<http://www.sbg.bio.ic.ac.uk/phyre2/>) supports a 6-TM model. Insertion sites of topology reporters are indicated as is the last residue modeled, K191.

Supplementary Table 1. MS/MS analysis of *MA-der1* N-terminal acetylation.

<i>MA-der1</i>				<i>nat3Δ</i>	<i>nat1-4</i>	WT
<u>peptide identified by mascot search</u>	<u>charge state</u>	<u>m/z</u>	<u>MH+</u>	<u>TIC max</u>	<u>TIC max</u>	<u>TIC max</u>
AAVILNLLGDIPLVTR	2	839.5192	1678.0384	1.11E+08	2.29E+08	1.70E+08
AAVILNLLGDIPLVTR	3	560.014	1678.042	2.21E+07	1.59E+07	8.33E+06
MAAVILNLLGDIPLVTR	2	905.037	1809.074	2.60E+06	2.20E+06	1.41E+06
M(ox)AAVILNLLGDIPLVTR	2	913.0377	1825.0754	8.66E+06	5.41E+06	4.78E+06
(ac)AAVILNLLGDIPLVTR	2	860.522	1720.044	7.08E+07	5.93E+06	1.24E+08
(ac)MAAVILNLLGDIPLVTR	2	926.0422	1851.0844		not seen	
(ac)M(ox)AAVILNLLGDIPLVTR	2	934.0397	1867.0794		not seen	
total TIC (+/- Met oxidation, +/-Met removal and +/- acetylation)				2.15E+08	2.58E+08	3.09E+08
total TIC for Met-removed peptides				2.04E+08	2.50E+08	3.02E+08
total TIC for acetylated + Met-removed peptides				7.08E+07	5.93E+06	1.24E+08
total for amino terminal peptide						
% of total peptides with Met removed				95%	97%	98%
% of total peptides acetylated (after Met removal)				35%	2%	41%

Supplementary Table 2. Yeast strains used in this study.

Name	Genotype	Source
BY4741	<i>MATa his3Δ1 leu2Δ0 ura3Δ0 met15Δ0</i>	Open Biosystems
BY4742	<i>MATα his3Δ1 leu2Δ0 ura3Δ0 met15Δ0</i>	Open Biosystems
MHY498	MHY501 with <i>ubc4Δ::HIS3</i>	Chen et al. (1993)
MHY500	<i>MATa his3-Δ200 leu2-3,112 ura3-52 lys2-801 trp1-1</i>	Chen et al. (1993)
MHY501	<i>MATα his3-Δ200 leu2-3,112 ura3-52 lys2-801 trp1-1</i>	Chen et al. (1993)
MHY1366	MHY500 with <i>prc1-1</i>	Biederer et al. (1997)
MHY1631	MHY501 with <i>doa10Δ::HIS3</i>	Swanson et al. (2001)
MHY1648	MHY501 with <i>doa10Δ::HIS3 ubc4Δ::HIS3</i>	Swanson et al. (2001)
MHY1661	MHY7719 with <i>ubc7Δ::HIS3</i> (RHY665)	Hampton & Bhakta (1997)
MHY1703	MHY501 with <i>doa10Δ::HIS3 hrd1Δ::LEU2</i>	Swanson et al. (2001)
MHY3032	BY4741 with <i>hrd1Δ::kanMX</i>	Open Biosystems
MHY3033	BY4741 with <i>doa10Δ::kanMX</i>	Open Biosystems
MHY3407	BY4741 with <i>nat3Δ::kanMX</i>	Open Biosystems
MHY6599	MHY501 with <i>nat3Δ::HIS3</i>	This study
MHY6623	BY4741 with <i>nat3Δ::kanMX ubc4Δ::kanMX</i>	This study
MHY6850	MHY501 with <i>ubc4Δ::HIS3 nat3Δ::HIS3</i>	This study
MHY6855	MHY500 with <i>hrd1Δ::HIS3 prc1-1</i>	This study
MHY6856	MHY501 with <i>doa10Δ::HIS3 nat3Δ::TRP1</i>	This study
MHY6920	MHY500 with <i>nat3Δ::HIS3 prc1-1</i>	This study
MHY7110	MHY500 with <i>der1Δ::kanMX6 prc1-1</i>	This study
MHY7111	MHY500 with <i>der1Δ::kanMX6 nat3Δ::HIS3 prc1-1</i>	This study
MHY7112	MHY500 with <i>der1Δ::kanMX6 mak3Δ::HIS3 prc1-1</i>	This study
MHY7428	BY4741 with <i>nat3Δ::kanMX</i>	A. Varshavsky
MHY7430	BY4741 with <i>nat3Δ::kanMX hrd1Δ::kanMX</i>	This study
MHY7432	MHY501 with <i>prc1-1 USA1-3myc::kanMX</i> (YTX625)	Horn et al. (2009)
MHY7690	MHY501 with <i>prc1-1 USA1-3myc::kanMX nat3Δ::TRP1</i>	This study
MHY7719	<i>MATα ade2-101 met2 lys2-801 his3Δ200 trp1::hisG ura3-52::6MYC-HMG2 hmg1Δ::LYS2 hmg2Δ::HIS3</i>	This study
MHY7720	MHY7719 with <i>nat3Δ::TRP1</i>	This study
MHY7794	MHY500 with <i>der1Δ::kanMX6 nat1-4::LEU2 prc1-1</i>	This study
MHY7834	MHY500 with <i>doa10Δ::HIS3 der1Δ::kanMX6</i>	This study

nat3Δ::TRP1 PRC1
MHY7839 MHY500 with *hrd1Δ::kanMX der1Δ::kanMX6* This study
nat3Δ::HIS3 prc1-1

Supplementary Table 3. Plasmids.

Name	Description	Source
pSM1911	<i>PGK1</i> promoter- <i>ste6-166-HAe</i>	Huyer et al. (2004)
pDA429	p416GPD-3HA-PCA1	Adle et al. (2008)
pDN431	CPY*-HA insert in YCp50	Ng et al. (2000)
pCAU-KHNt	KHN reporter in YCp50	Vashist et al. (2001)
pDA457	<i>NAT3</i> gene in pRS416	This study
pSZ1	<i>UPRE-lacZ</i> in 2 μ m/URA3 plasmid	Friedlander et al. (2000)
p415GPD-DER1-HA	<i>DER1-HA</i> inserted into p415GPD	This study
p415-DER1-HA	<i>GPD</i> promoter of p415GPD-DER1-HA replaced with 500- bp <i>DER1</i> promoter	This study
p415-der1-D2X-HA	X=S,L,E,A, or K, ; Der1 second codon changes in p415-DER1-HA	This study
p414-DER1-HA	XhoI-SacI insert from p415-DER1-HA subcloned into pRS414	This study
p414-der1-D2A-HA	XhoI-SacI insert from p415-der1-D2A-HA subcloned into pRS414	This study
p415MET25-Deg1-F-URA3	<i>Deg1-URA3</i> with FLAG (F) insertion	This study
p416GPD-DER1-FLAG	XbaI-XhoI PCR fragment of <i>DER1-FLAG</i> inserted into p416GPD	This study
p416GPD-der1D2A-FLAG	XbaI-XhoI PCR fragment of der1D2A-FLAG inserted into p416GPD	This study
p415MET25 DER1	XbaI-XhoI PCR fragment of <i>DER1</i> ORF inserted into p415MET25	This study
p415-DER1	MET25 promoter of p415MET25 DER1 was replaced by SacI-XbaI PCR fragment with 500 bp <i>DER1</i> promoter	This study
p415-DER1-FLAG	XbaI-XhoI PCR fragment of <i>DER1-FLAG</i> was inserted into p415-DER1	This study
p416GPD Der1 D45::SUC2A-FLAG	pHIT124 from Hitt et al., 2004 was used as template to amplify the DER1 D45::SUC2A ORF as a FLAG-tagged XbaI-XhoI PCR fragment and then inserted into p416GPD	This study

p416GPD Der1
E85::SUC2A-FLAG

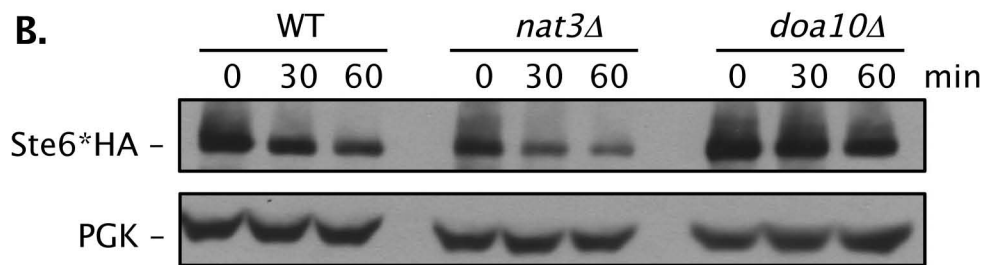
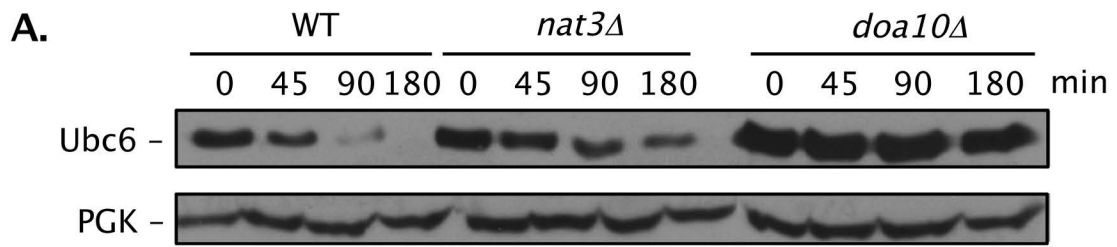
pHIT125 from Hitt et al., 2004 was used as
template to amplify the DER1 E85::SUC2A ORF
as a FLAG-tagged XbaI-XhoI PCR fragment and
then inserted into p416GPD

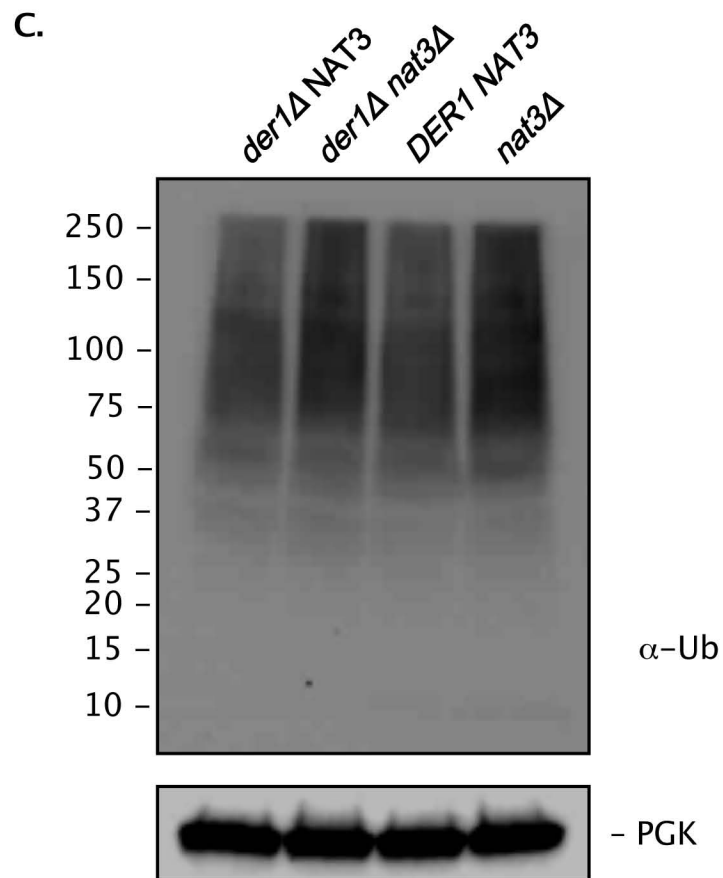
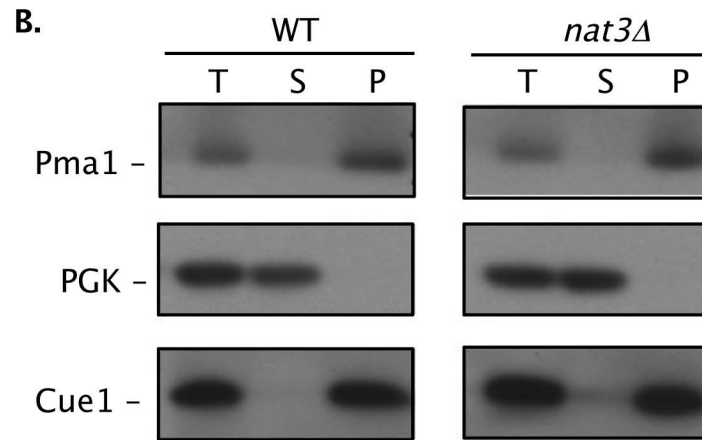
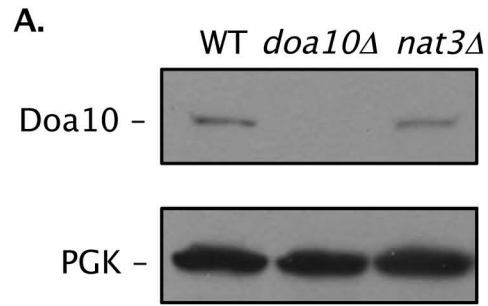
This study

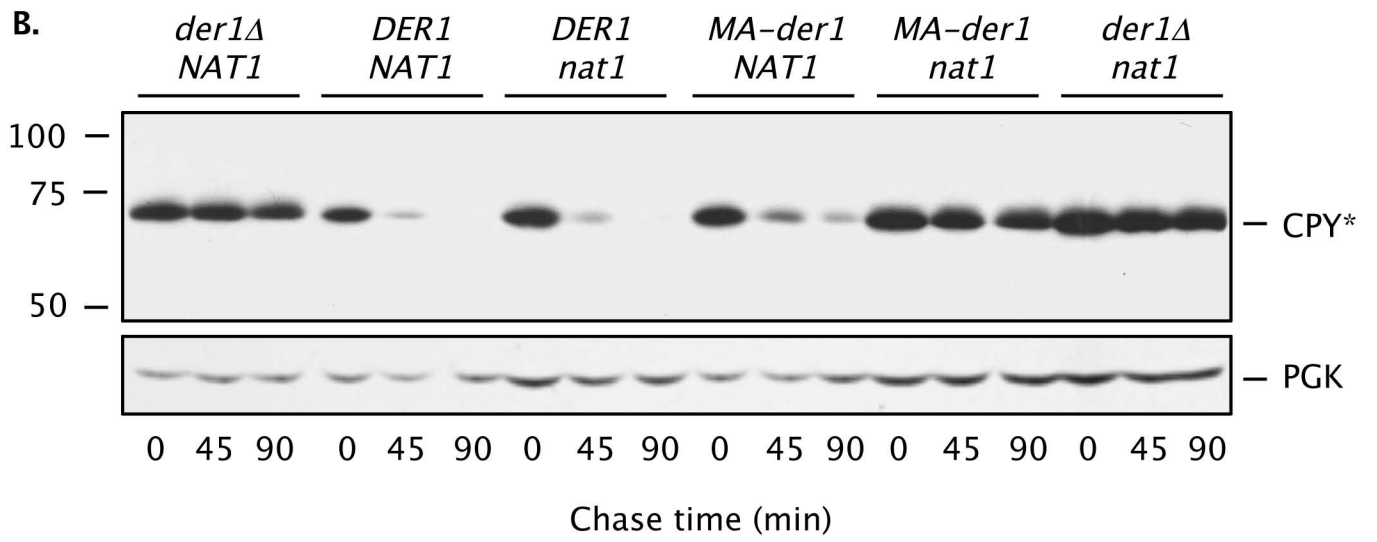
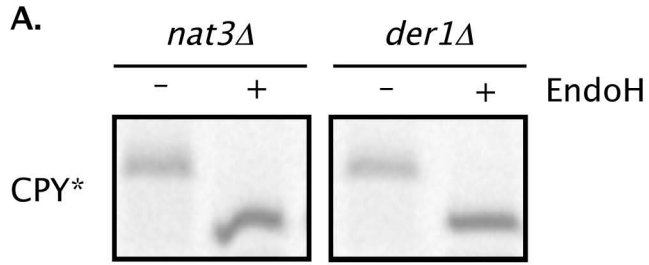
p416GPD Der1
Y128::SUC2A-FLAG

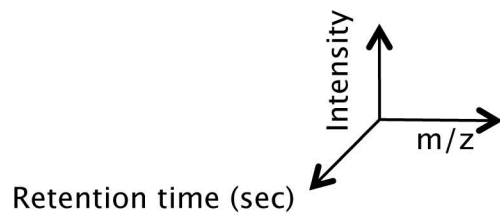
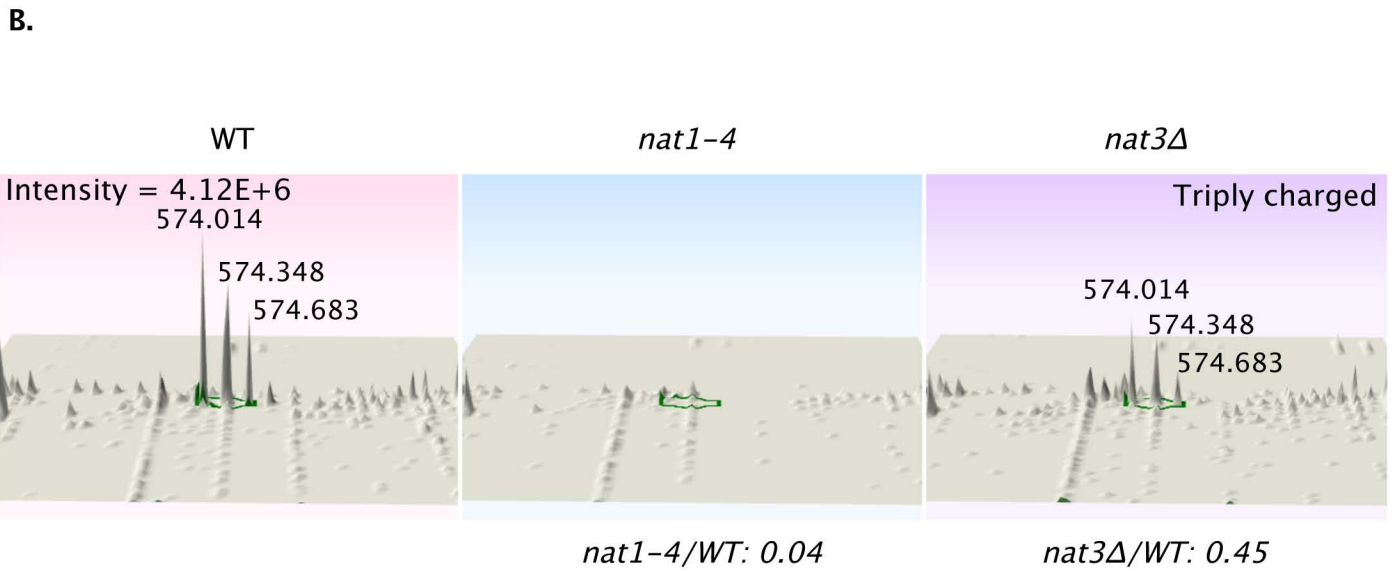
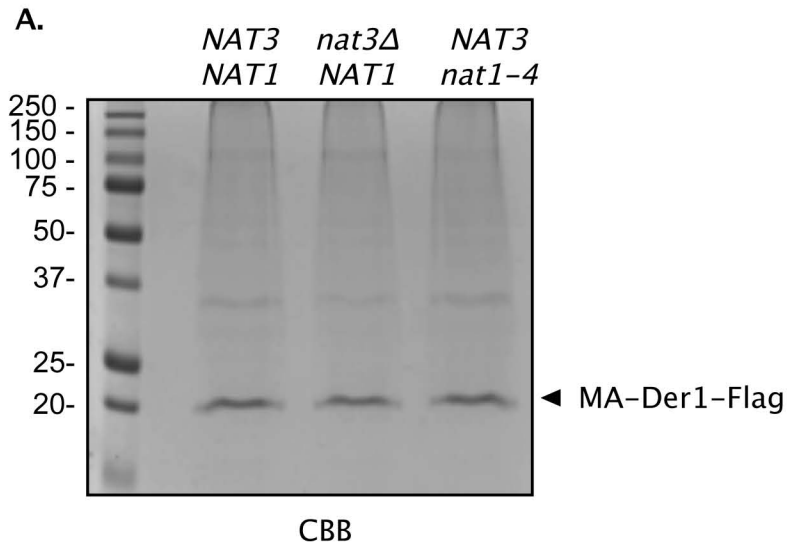
pHIT126 from Hitt et al., 2004 was used as
template to amplify the DER1 Y128::SUC2A ORF
as a FLAG-tagged XbaI-XhoI PCR fragment and
then inserted into p416GPD

This study

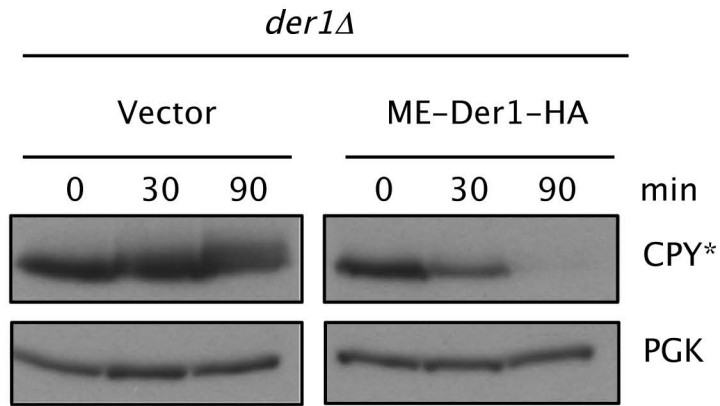




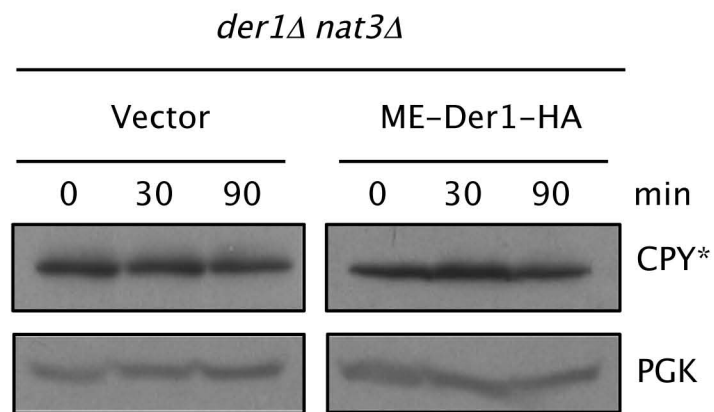




A.



B.



C.

